Successive antiferromagnetic phase transitions in single-crystal La_2CoO_4

K. Yamada,* M. Matsuda, and Y. Endoh
Department of Physics, Tohoku University, Aramaki Aoba, Sendai 980, Japan

B. Keimer* and R. J. Birgeneau
Department of Physics, Massachusetts Institute of Technology, Cambridge, Massachusetts 02139

S. Onodera
Sendai National College of Technology, Sendai 989-31, Japan

J. Mizusaki
Institute of Environmental Science and Technology, Yokohama National University, Tokiwadai, Hodogaya-ku, Yokohama 240, Japan

T. Matsuura
Research Institute of Electrical Communication, Tohoku University, Katahira, Sendai 980, Japan

G. Shirane
Brookhaven National Laboratory, Upton, New York 11973
(Received 21 September 1988)

We have observed successive magnetic phase transitions in a La_2CoO_4 single crystal by neutron scattering measurements. Antiferromagnetic long-range order of the La_2NiO_4 type, τ[100], **S**[100], is observed with Néel temperature $T_N = 275$ K in the orthorhombic (*Cmca*) phase. As the temperature is lowered, a first-order phase transition to a new tetragonal phase is found at $T_2 \sim 135$ K. This structural phase transition is accompanied by a Co^{2+} ($S = \frac{3}{2}$) spin rotation or flip in the CoO_2 plane which results in a new spin structure with the spin direction **S** perpendicular to τ, the propagation vector of the antiferromagnetic structure. The spin direction itself of this phase cannot be determined uniquely due to the tetragonal symmetry and indeed the most likely structure is noncollinear. In contrast to the $S = \frac{1}{2}$ Heisenberg system La_2CuO_4, well-defined, two-dimensional Ising critical phenomena are observed and the two-dimensional spin correlations at $T > T_N$ are almost entirely elastic.

I. INTRODUCTION

Extensive neutron scattering studies on pure and Sr-doped La_2CuO_4 compounds[1-3] have been carried out since the discovery of superconductivity in $La_{2-x}Ba_xCuO_4$.[4] These studies are important for our understanding of the superconductivity, first because they have evinced a large energy scale for the in-plane exchange couplings between Cu^{2+} spins, and second because they have also revealed various new and interesting properties characteristic of the spin-$\frac{1}{2}$, two-dimensional (2D), Heisenberg antiferromagnet. In order to elucidate further the possible relationship between the dynamical spin fluctuations and the superconductivity, it is necessary to refine our understanding of the magnetism in such lamellar oxide systems. Most importantly, in order to understand which properties are unique to the $S = \frac{1}{2}$ 2D Heisenberg nature of La_2CuO_4 it is essential that one investigate the magnetism of isomorphous oxides with transition metals other than Cu.

A neutron scattering study of La_2CoO_4, one of the isomorphous compounds of La_2CuO_4, was initiated using the pulsed neutron source at the National Laboratory for High Energy Physics (KEK) in Japan. In these measurements, a structural phase transition from orthorhombic-to-tetragonal symmetry was found around $T = 135$ K with decreasing temperature. As will be discussed below, in further measurements at Brookhaven National Laboratory, we discovered two magnetic phases as well as a new tetragonal structure qualitatively different from the high-temperature tetragonal one. In the early stages of this work, we were informed of a similar structural change to a tetragonal phase observed in ceramic $La_{2-x}Ba_xCuO_4$.[5] Also, at the beginning of our study, we learned of the experimental results of magnetic neutron scattering measurements carried out on La_2NiO_4.[6] Therefore, we are now able to compare in more detail these three isomorphous systems with Cu, Ni, and Co ions. As we shall discuss below these ions have, respectively, $S = \frac{1}{2}$, $S = 1$, and $S = \frac{3}{2}$.

The structure of these compounds is determined in good part by the MO_6 octahedra and their tilts (M represents a $3d$ metal). Summarizing the previous studies, we show schematically in Fig. 1 the temperature dependence of the in-plane lattice constant. The high-temperature tetragonal phase ($I4/mmm$) transforms to a lower temperature orthorhombic one (*Cmca*) at $T = T_1$. This phase transition has been found to be caused by the softening of one of

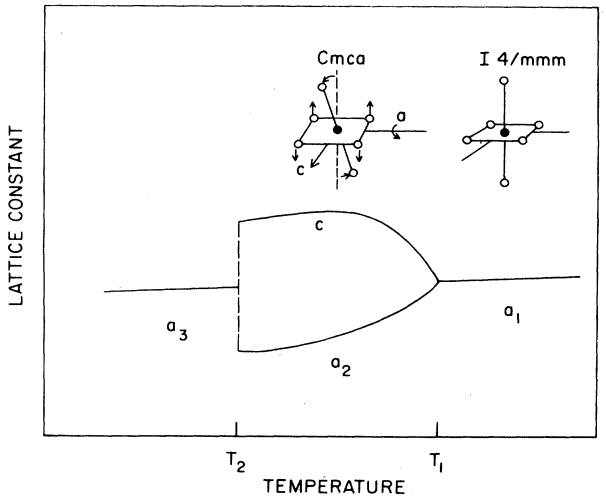

FIG. 1. Schematic illustration of the temperature dependence of the lattice constants in the MO_2 plane for an La_2MO_4 compound.

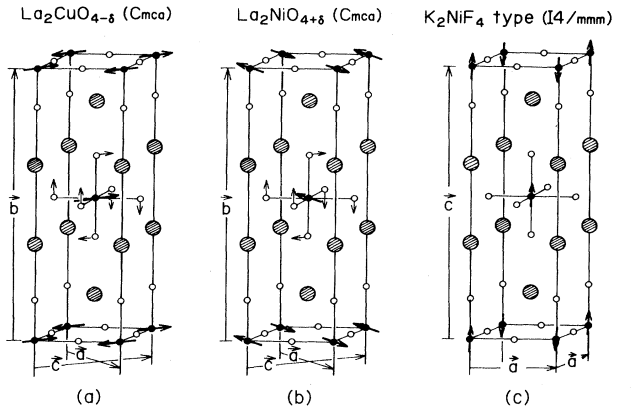

FIG. 2. Two types of spin structures and the tilt of octahedron in the orthorhombic La_2MO_4 compound. Closed, open, and hatched circles denote M, O, and La atoms, respectively.

the zone-boundary TO modes which is doubly degenerate in the tetragonal phase.[7,8] The second tetragonal phase below T_2 is less well understood. However, in the analogous system $(CH_3NH_3)_2MnCl_4$ structural studies give the space group as $P4_2/ncm$; this is characterized by a rotation of the octahedra about a tetragonal axis.[9] Recently, the softening of the second rotational mode of the octahedron has been proposed[5] as the driving mechanism for this phase transition from *Cmca* to $P4_2/ncm$ symmetry.

Neutron scattering studies performed on these lamellar transition-metal oxides have so far revealed two types of antiferromagnetic spin structures in the orthorhombic *Cmca* phase; one is the La_2CuO_4 type, τ[100], **S**[001];[10,11] and the other is the La_2NiO_4 type,[6] τ[100], **S**[100], where **S** and τ denote the spin direction and antiferromagnetic propagation vector, respectively. $\tau \| [100]$ follows from the fact that $a < c$ and the basic interplanar interaction is antiferromagnetic; these two spin structures are illustrated in Fig. 2. The structures are interchangeable by a rotation of the spin by 90° about the b axis. Recently, however, a slight cant of the spin towards the b axis by $\sim 0.17°$ has been determined for the Cu compound[12,13] due to the antisymmetric exchange interaction which originates from the tilt of the octahedra.[13] A magnetic phase transition at high magnetic field to a structure with τ[010], **S**[001] has been both predicted and observed for the Cu compound.[14]

The temperature dependence of the static magnetic susceptibilities is similar in both La_2CuO_4 (Refs. 13, 15, and 16) and in at least one sample of La_2NiO_4 (Ref. 17), where a pronounced peak has been observed at T_N when the external field is applied perpendicular to the MO_2 planes. The sharpness of the peak as well as the phase transition temperature T_N itself is very sensitive to deviations of the oxygen content from stoichiometry. The antisymmetric interaction combined with the temperature dependence of the 2D spin-correlation length can quantitatively explain the susceptibility peak of the Cu compound around T_N.[13] The peak observed in La_2NiO_4 remains unexplained, although it is possible that in the actual sample studied the magnetic structure was of the La_2CuO_4 type.

In the Co compound, the susceptibility measurements published to date have been performed only for powdered samples and are rather inconclusive. A sharp peak at 405 K and a broad hump centered around 500 K have been reported.[18,19] The former is sensitive to the oxygen content and observed only in the crystal with higher oxygen content. On the other hand, the latter is almost independent of the oxygen content. The authors interpreted these two peaks in terms of 3D antiferromagnetic order and 2D spin correlations, respectively. Alternatively, a possible transition between the high-spin ($S = \frac{3}{2}$) and the low-spin state ($S = \frac{1}{2}$) of the Co^{2+} ion has been proposed as an explanation of the change in the slope of the inverse susceptibility observed around 400 K.[20]

In this paper we present neutron scattering measurements performed on a La_2CoO_4 *single crystal* which clarify a number of the salient issues. The format of this paper is as follows. Following a brief description of the experimental technique (Sec. II), the structural phase transition at T_2 is reported in Sec. III. The successive antiferromagnetic transitions are surveyed in Sec. IV. In Sec. V we discuss the spin state of the Co^{2+} ion in this compound as well as the relationship between the spin structure and the low-temperature tetragonal phase.

II. EXPERIMENTAL TECHNIQUE

A single crystal of La_2CoO_4 was prepared by a floating-zone method from stoichiometric powder material synthesized by the coprecipitation method.[21] This method is known to yield more homogeneous and stoichiometric specimens than those obtained from the direct calcination of the mixture of La_2O_3 and CoO in vacuum. The melting and annealing were done in a CO/CO_2 atmosphere in order to preserve the oxygen stoichiometry. An x-ray

powder-diffraction analysis revealed no impurity phase in the single crystal. Although we did not determine the precise concentration of oxygen in the present crystal, the lattice constants determined by x-ray diffraction (crystal G in Table I) are in excellent agreement with those of stoichiometric crystal (crystal F in Table I).[19]

The neutron scattering measurements were carried out using the triple-axis spectrometers H4M, H9, and H7 at the Brookhaven High Flux Beam Reactor. The crystal, which has dimensions of 4 mm in radius and 10 mm in height, was mounted with an $\mathbf{a}^*$ (or $\mathbf{c}^*$) axis vertical in an Al can in which He gas was contained as a heat exchanger. The Al can was attached to the cold finger of a liquid-N_2 flow cryostat. Because of the twin structure in the orthorhombic phase, the a^* and c^* axes are superposed. For measurements in the low-temperature phase, the Al can was remounted with $\mathbf{b}^*$ vertical to allow scans in the tetragonal $\mathbf{a}^*$-$\mathbf{c}^*$ reciprocal-lattice plane. Different energy incident neutrons together with different horizontal collimations were utilized to optimize the various types of measurements. In order to eliminate contamination by higher-order neutrons, a beryllium filter cooled down to 77 K or a pyrolytic graphite filter was inserted in the incident or the scattered neutron beam path. The temperature of the crystal was monitored by a platinum resistance thermometer and controlled to within ± 0.1 K.

Before considering the actual data, it is essential to understand the distribution of Bragg points in the reciprocal-lattice plane. In Fig. 3 we show the nuclear and magnetic Bragg reflections in an $\mathbf{a}^*(\mathbf{c}^*)$-$\mathbf{b}^*$ reciprocal-lattice plane of the orthorhombic twin structure. The open and closed circles denote the primary and superlattice nuclear reflections, respectively, while the triangles show the magnetic Bragg reflections. In the Ni- (Cu-) type structure, the spin direction is along $\mathbf{a}^*$ ($\mathbf{c}^*$) and parallel (perpendicular) to the scattering plane for one of the twin crystals shown by closed triangles and perpendicular (parallel) to the other shown by the open ones.

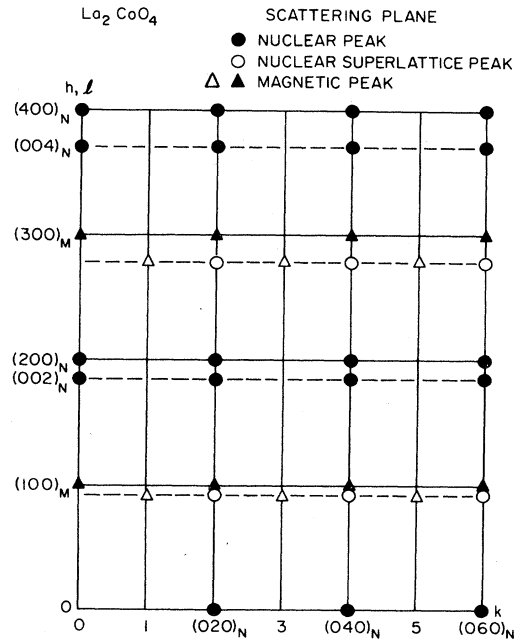

FIG. 3. Reciprocal $a^*(c^*)$-b^* planes superposed by the twinned structure. Open and closed circles denote nuclear and nuclear superlattice reflections, respectively. Open and closed triangles denote magnetic reflections with the spin directions perpendicular to each other (see text).

III. CRYSTAL STRUCTURE

Previous measurements[19,22–26] show that the room-temperature lattice constants of La_2CoO_4 in the orthorhombic phase vary drastically for different crystals as shown in Table I. Among the samples studied, the present crystal G has the maximum orthorhombic distortion. In Fig. 4 we show the temperature dependences of the lattice constants a, b, and c in our crystal. At $T_2 \sim 135$ K, a first-order structural phase transition occurs with discontinuous changes in a and c but not in b. We performed high-Q resolution measurements ($\delta Q \simeq 0.013$ Å^{-1} full width at half maximum) in the tetragonal $(H,K,0)$ zone below T_2 and confirmed the tetragonality of the low-temperature phase. As will be described in the next section, this phase transition is accompanied by a change in the magnetic structure. However, the transition does not go to completion; in both phases there remains a small amount ($\sim 5\%$) of the residual orthorhombic (tetragonal) phase in the low- (high-) temperature one, which prohibits an accurate refinement of the structural parameters.

We performed θ-2θ scans to measure the integrated intensities of several Bragg peaks including superlattice and magnetic ones above ($T = 150$ K) and below ($T = 80$ K) T_2. Above T_2, as shown in Fig. 5, these intensities are well described by the structural parameters of *Cmca* obtained from the previous study on crystal J in Table I where the angle Φ of the tilt of octahedron is about 0.8°. Here, we adjusted the parameters to increase the angle Φ as required by the larger orthorhombic distortion. The tilt angle Φ of $\sim 10°$ obtained in this analysis is about 2.5 times larger than that of the Cu compound ($\Phi \sim 4.2°$). A similar, albeit less drastic, difference is found for the or-

TABLE I. Lattice constants of $La_{2-x}CoO_{4+y}$.

Crystal	a (Å)	c (Å)	b (Å)
A[a]	5.473	5.538	12.57 (Ref. 25)
B[b]	5.484	5.550	12.67 (Ref. 25)
C[c]	5.471	5.606	12.65 (Ref. 25)
D[d]	5.476	5.526	12.650 (Ref. 19)
E[e]	5.493	5.543	12.684 (Ref. 19)
F[f]	5.474	5.614	12.648 (Ref. 19)
G	5.4733	5.6064	12.656 (Ref. 22)
H	5.525	5.599	12.64 (Ref. 23)
I	5.474	5.530	12.65 (Ref. 23)
J	5.488	5.490	12.548 (Ref. 26)
K	5.470	5.530	12.55 (Ref. 24)

[a] $La_{1.83}CoO_4$.
[b] $La_{1.83}CoO_{3.875}$.
[c] $La_{1.83}CoO_{3.75}$.
[d] $La_2CoO_{4.11}$.
[e] $La_2CuO_{4.10}$.
[f] $La_2CoO_{4.00}$.

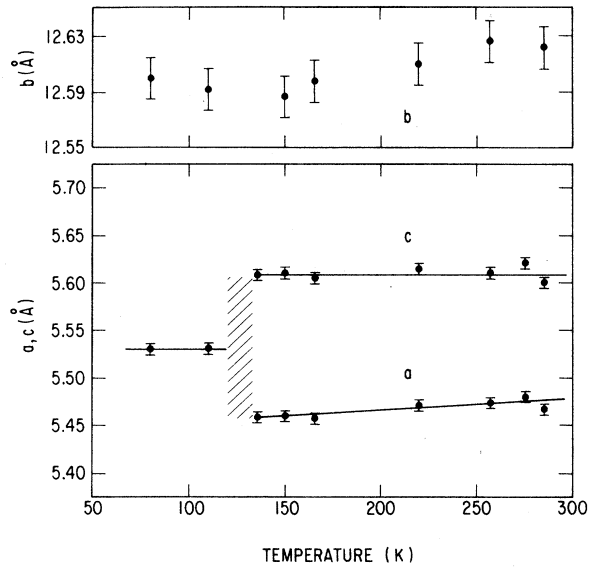

FIG. 4. Temperature dependence of the lattice constants of La_2CoO_4. The hatched region shows the mixed phase of the tetragonal and the orthorhombic structure.

thorhombic distortion in the two compounds: $(c-a)/(c+a)=1.3\times10^{-2}$ for the Co compound (150 K) and 0.71×10^{-2} for the Cu compound (10 K).[22,27]

Below T_2, the observation of the superlattice reflections requires a tetragonal unit cell with in-plane dimensions $\sqrt{2}\times\sqrt{2}$ of those of the high-temperature tetragonal structure ($I4/mmm$). A quantitative structural refinement shows that the space group $P4_2/ncm$ is likely for this phase although our data are too sparse to make a unique assignment.

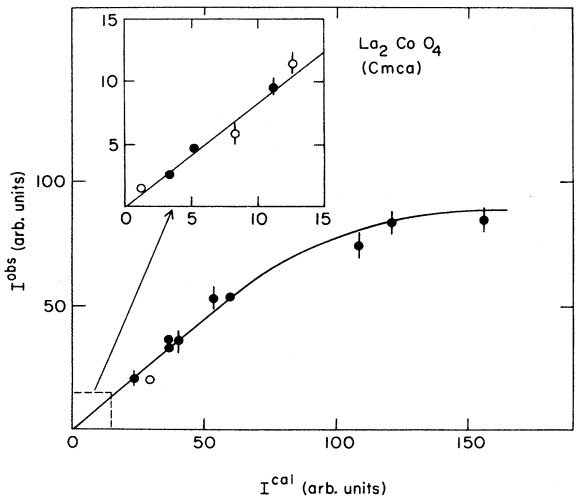

FIG. 5. The calculated and the observed nuclear intensities of our La_2CoO_4 single crystal in the high-temperature orthorhombic ($Cmca$) phase. Open circles denote superlattice reflections.

IV. SUCCESSIVE PHASE TRANSITIONS

In Fig. 6 we show the overall temperature dependences of the magnetic Bragg peak intensities at the (100) and (011) reciprocal-lattice positions (see Fig. 3) and those at "off Bragg" points along the 2D magnetic ridge of $(0,K,1)$. Figure 6(a) clearly shows the successive phase transitions in this system. Above T_N, where there is no 3D magnetic order, we observe magnetic quasielastic scattering corresponding to the 2D spin correlations in the CoO_2 planes, similar to those observed previously in many 2D systems.[28] Between T_2 and T_N (hereafter we call this region phase I and the region $T<T_2$, phase II), the spin structure is found to be identical to that of La_2NiO_4 with τ[100], S[100]. Around T_2, a crossover of the intensities of [011] and [100] takes place. In phase II, the magnetic Bragg intensities for peaks which are uncontaminated by nuclear superlattice scattering can be explained by assuming a La_2CuO_4-type spin structure (Table II) τ[100], S[001]. It is noted that the Cu-type spin structure can be constructed from the Ni type by a 90° spin rotation or a flip of the spin on half of the CoO_2 planes. As we shall discuss in Sec. V, because of the tetragonal symmetry, more general noncollinear structures derived from the La_2CuO_4 structure are also allowed by the data. The magnetic moments of the Co^{2+} ions are identical in both phases within the experimental resolution. We find for the moment a value of $(2.9\pm0.1)\mu_B$ which corresponds to that of Co^{2+} in the high-spin state ($S=\frac{3}{2}$) assuming

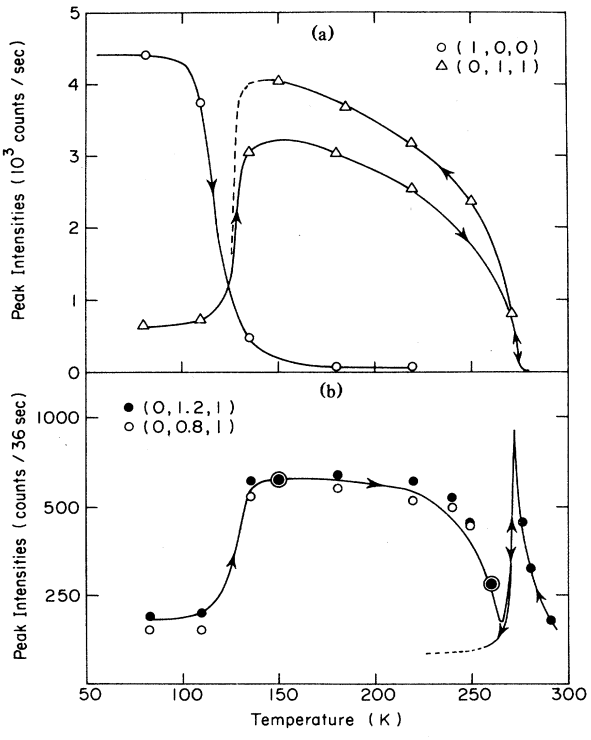

FIG. 6. (a) Temperature dependences of the (1,0,0) and (0,1,1) peak intensities and (b) those at the "off Bragg" points of (0,1.2,1) and (0,0.8,1) on the 2D magnetic ridge $(0,K,1)$.

TABLE II. Observed and calculated relative intensities of magnetic Bragg reflections at $T=80$ K (phase II) and $T=150$ K (phase I).

	Phase II ($T=80$ K)		Phase I ($T=150$ K)	
(hkl)	I^{obs}	I^{cal}	I^{obs}	I^{cal}
100	103	104	<2.4	0
011	20.5	16.0	100	100
120	95.9	92.2	39.8	39.6
031	50.3	50.5	84.2	82.2
140	a	70.7	60.9	53.6
051	58.8	49.8	73.7	61.4
160	a	50.0	· · ·	44.0
300	49.8	46.0	· · ·	0
013	b	0.9	40.7	45.0
033	b	6.2	33.4	39.9
071	49.8	36.0	49.0	40.4
340	a	34.6	8.5	7.7

[a]Superposed by superlattice reflections.
[b]Contaminated by residual (Ni-type) phase.

$g\simeq 2$. We note that this moment is reduced from its bare value by zero-point effects. The true value is probably closer to $(3.25\pm 0.15)\mu_B$, a value somewhat larger than $3\mu_B$ and consistent with the XY-like symmetry of the Co^{2+} spin. The Q dependence of the magnetic Bragg intensities also follows the magnetic form factor of the Co^{2+} ion determined by CoO.[29]

The Ni-type spin structure persists in the residual orthorhombic structure in phase II. On the other hand, in the residual tetragonal phase in phase I, there appears to be no magnetic long-range order.

In phase I we observe a dramatic hysteresis in the magnetic intensities when we reenter this phase by heating the crystal from phase II. The peak intensities of the magnetic Bragg reflections are considerably reduced compared with those obtained on cooling. This missing intensity appears as strong diffuse scattering along the b^* direction, that is, in the form of a 2D rod. The huge difference of the scattered neutron spectra between heating and cooling processes is shown in Fig. 6(b). This thermal hysteresis entirely disappears in the vicinity of T_N. This hysteresis undoubtedly derives from stacking faults in the La_2CoO_4 magnetic structure which are generated at the first-order transition on heating from phase II to phase I. These stacking faults then anneal out near T_N.

From the temperature dependence of the (011) Bragg intensity (Fig. 7), we determined the Néel temperature T_N to be 274.7 ± 0.6 K. As noted above, for $T>T_N$, the system exhibits 2D fluctuations. As shown in Fig. 8(a), along the 2D magnetic ridge $(0,K,1)$, significant 2D intensity is observed with little indication of 3D short-range-order effects. The latter become observable only near T_N. For scans across the ridge, we observe well-defined peaks (Fig. 9) corresponding to a long 2D spin correlation length. In La_2CuO_4, an unusually high inelasticity is associated with these 2D spin fluctuations.[1] No such effect is observed in La_2CoO_4. Indeed, as shown in Fig. 10, the energy spectrum of the constant-Q scan on the ridge is very sharply peaked around $\Delta E=0$. La_2CoO_4

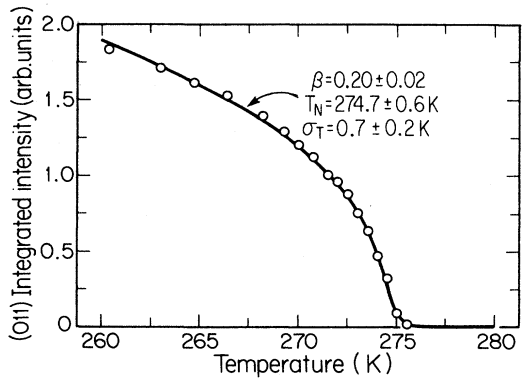

FIG. 7. Integrated intensity of the (011) magnetic reflection near T_N; the solid line is the result of a least-squares fit to a simple power law with a Gaussian distribution of Néel temperatures as discussed in the text.

also exhibits a clear contrast to La_2CuO_4 in the temperature dependence of the instantaneous 2D correlation function $[S(\mathbf{Q}_{2D})]$,

$$S^{aa}(\mathbf{Q}_{2D})=\int_{\infty}^{-\infty} d\omega\, S^{aa}(\mathbf{Q}_{2D},\omega)\,. \tag{1}$$

Here $\mathbf{Q}_{2D}$ is the component of the momentum transfer in the MO_2 planes. When the energy integration of Eq. (1) is properly performed within the static approximation, the intensity of a double-axis scan with the scattered neutron momentum $\mathbf{k}_f$ perpendicular to the 2D magnetic

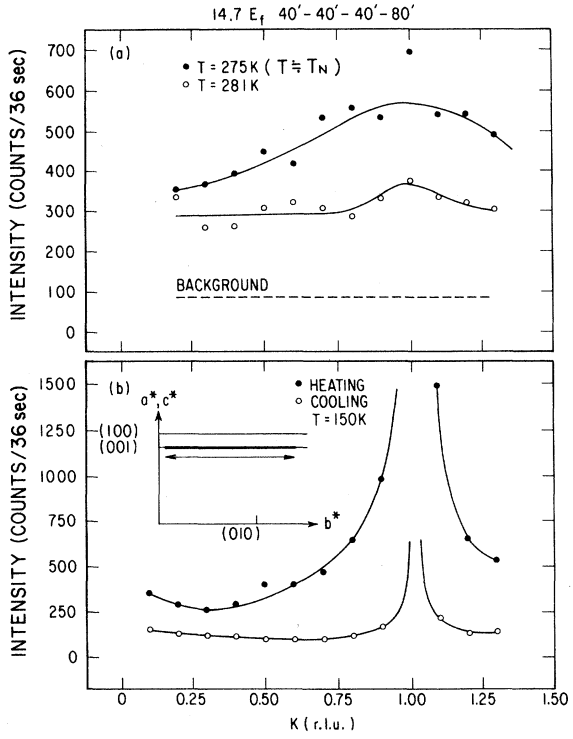

FIG. 8. Elastic parallel scans along the 2D magnetic ridge at several temperatures.

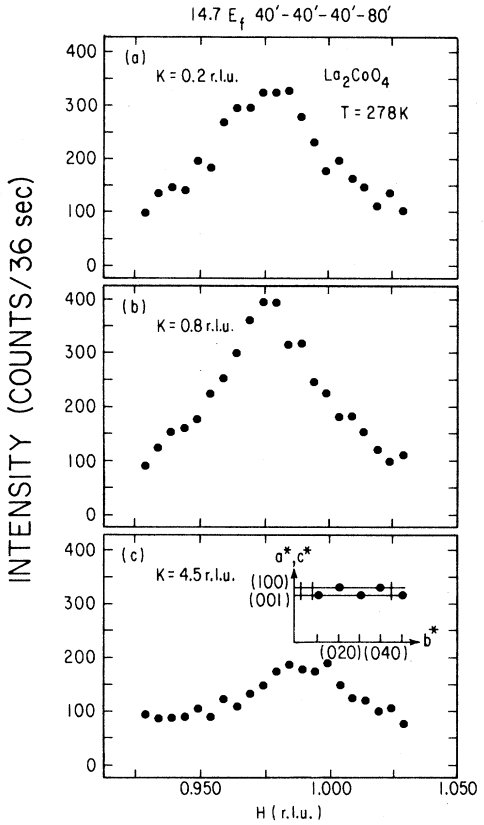

FIG. 9. Elastic transverse scans across the 2D magnetic ridge at $K=0.2$ (a),0.8 (b), and 4.5 (c).

plane provides $S(\mathbf{Q}_{2D})$. The peak intensity $S(\mathbf{Q}_{2D}=0)$ on the ridge shows a very sharp peak at T_N in good accord with the observed critical behavior in the typical 2D Ising systems such as K_2CoF_4,[30] K_2NiF_4,[28] and La_2NiO_4.[6] The 2D Ising character also manifests itself in the intensity profiles of the scans across the ridge (Fig. 9). For small K, we observe a peak centered around the $(O,K,1)$ ridge but not the $(1,K,0)$ ridge; for the latter we cannot detect

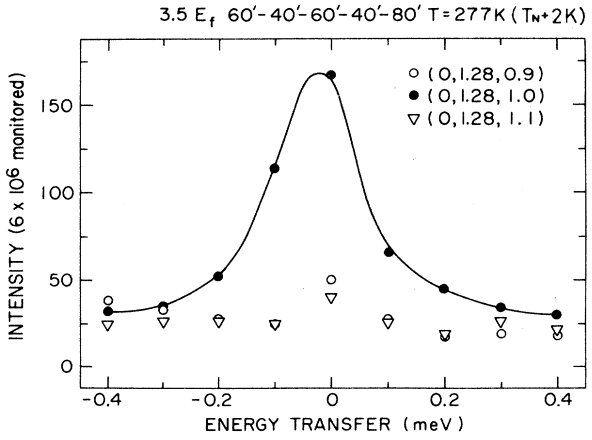

FIG. 10. Energy scans around 2D magnetic ridge $(0,K,1)$ in the constant-Q mode.

the longitudinal component of the spin correlations because the spin direction is parallel to the scattering vector. This demonstrates that the spin correlations in this compound are dominated by the longitudinal Ising component.

All of the above features are in contrast to the behavior observed in La_2CuO_4. In the Cu system the fluctuations are highly inelastic, have at least XY symmetry, and show no obvious divergent behavior at T_N. We assume that this is because of the predominant 2D, $S=\frac{1}{2}$, Heisenberg character of La_2CuO_4 and the fact that the transition to long-range order is driven by the interplanar coupling rather than the Ising anisotropy.

Finally, we show in Fig. 7 the results of a least-squares fit of a simple power law, $I=A(1-T/T_N)^{2\beta}$, convoluted with a Gaussian distribution $\{\exp[-(\Delta T/\sigma_T)^2]\}$ of Néel temperatures. Clearly, the simple power law with an appropriately "smeared" T_N describes the data quite well. The best-fit parameters are $\sigma_T=0.7\pm0.2$ K and $\beta=0.20\pm0.02$. The latter may be compared with $\beta=0.125$ for the 2D Ising model, 0.14 ± 0.01 in K_2NiF_4 and 0.16 ± 0.02 in Rb_2MnF_4.[28] Thus the behavior is closer to 2D than 3D ($\beta\simeq0.33$) in character, although the intermediate value for β suggests that the measurements span the crossover regime from 3D to 2D behavior.

V. DISCUSSION

The present measurements show that the majority of Co ions stays in the divalent high-spin states in both phase I and phase II. We did not detect Co^{3+} ions due to the excess oxygen or lanthanum deficiency within our experimental resolution (~6%). Also, there is no high-spin–low-spin transition between 77 and 290 K as was predicted from one of the uniform susceptibility measurements on a powder sample.[20] These results are, however, consistent with the model proposed from systematic studies of the transport properties and the lattice constants on the $La_{2-x}Sr_xCoO_4$ single crystals.[22,31] There, all of the Co ions in undoped La_2CoO_4 crystal have been presumed to be divalent and to stay in the high-spin state.

So far, there is only limited information on the spin Hamiltonian relevant to the Co^{2+} ions in La_2CoO_4. We may, nevertheless, deduce a number of basic features from our neutron scattering experiments together with results from some preliminary single-crystal susceptibility measurements. First, the bulk susceptibility between 300 and 440 K is characteristically 2D with the in-plane value about 50% larger than that out of plane. This suggests that the spins predominantly lie in the planes and, in the absence of in-plane anisotropy, would be described by an XY model. The in-plane symmetry is broken by the rotation of the CoO_6 octahedra as in La_2CuO_4. However, in the Co case the spin is parallel to the rotation axis and hence also parallel to the antisymmetric exchange vector $\mathbf{D}$. This requires that either effective crystal field or anisotropic exchange effects control the in-plane anisotropy. This intraplanar anisotropy clearly predominates over the interplanar exchange interaction, hence accounting for the 2D Ising character of the phase transition.

As an aside, it should be noted that the $S=\frac{3}{2}$ character

of the Co^{2+} ion means that electrons are removed successively from the $d_{x^2-y^2}$, $d_{3z^2-r^2}$, and d_{xy} orbitals. Thus the intra-atomic Hund's rule coupling predominates over the crystal field. This has an interesting consequence for models of the electronic structure of La_2CuO_4. Specifically, this hierarchy of the energy levels will serve to stabilize holes in the nonbonding oxygen π orbitals, since it costs less energy to transfer a hole from the O^- site to the Cu^{2+} site through either a d_{xy} orbital or a $d_{3z^2-r^2}$ orbital. The relative efficiency of the two possible π orbitals will be determined by the relevant transfer integrals.[32,33]

Next we discuss the low-temperature tetragonal phase. As noted above, if we assume a collinear spin structure, then the spins order in the simple La_2CuO_4 magnetic structure illustrated in Fig. 2(a). However, a more elaborate noncollinear structure seems more likely. As noted above, in phase I, the rotation of the CoO_6 octahedra uniquely determines the spin direction. However, in the low-temperature tetragonal structure which we assume to have the $P4_2/ncm$ structure, the octahedra rotate about alternate tetragonal axes layer by layer. Thus the spin direction may also rotate back and forth by 90° in alternate layers. This spin structure is obtained simply by combining coherently the magnetic structure shown for La_2CuO_4 in Fig. 2(a) with the equivalent structure with all spins rotated by 90°.

In summary, we have found successive antiferomagnetic phase transitions in an La_2CuO_4 single crystal. The La_2NiO_4-type spin structure in the high-temperature orthorhombic phase transforms to the La_2CuO_4 type by the Co^{2+} spin rotation or flip within the plane in the low-temperature tetragonal phase. A spin structure with spin rotations alternating by 90° between the CoO_2 planes but with the basic symmetry of the Cu-type structure is possible in this 2D Ising system.

From the point of view of lattice dynamics, two possible rotational modes of the octahedron which result in a tetragonal structure may go soft at the transition temperature. A rotation about **c** staggered along **a** corresponds to the softening of the second mode proposed for the structural transition of $La_{2-x}Ba_xCuO_4$ at T_2.[5] A twisted rotation about [101] is another candidate for this structural transition. These two types of modifications from *Cmca* can be distinguished by the different behavior of any possible phonon softening at the transition and differences in the possible intermediate orthorhombic phase. Thus to understand phase II fully both a determination of the space group and refinement of the structural parameters for the low-temperature phase as well as a study of the phonons associated with this phase transition are required.

ACKNOWLEDGMENTS

We wish to acknowledge stimulating discussions with Amnon Aharony, J. D. Axe, D. E. Cox, T. Freltoft, M. A. Kastner, T. R. Thurston, and J. M. Tranquada. This work was supported by the U.S.-Japan Cooperative Neutron Scattering Program and a Grant-In-Aid for Scientific Research from Japanese Ministry of Education, Science and Culture. Research at Brookhaven National Laboratory was supported by the division of Materials Science, U.S. Department of Energy under Contract No. DE-AC02-76Ch00016. Work at MIT was supported by the National Science Foundation under Contract No. DMR85-01856.

*Present address: Brookhaven National Laboratory, Upton, NY 11973.

[1]G. Shirane, Y. Endoh, R. J. Birgeneau, M. A. Kastner, Y. Hidaka, M. Oda, Y. Enomoto, M. Suzuki, and T. Murakami, Phys. Rev. Lett. **59**, 1613 (1987).

[2]Y. Endoh, K. Yamada, R. J. Birgeneau, D. R. Gabbe, H. P. Jenssen, M. A. Kastner, C. J. Peters, P. J. Picone, T. R. Thurston, J. Tranquada, G. Shirane, Y. Hidaka, M. Oda, Y. Enomoto, M. Suzuki, and T. Murakami, Phys. Rev. B **37**, 7443 (1988).

[3]R. J. Birgeneau, D. R. Gabbe, H. P. Jenssen, M. A. Kastner, P. J. Picone, T. R. Thurston, G. Shirane, Y. Endoh, M. Sato, K. Yamada, Y. Hidaka, M. Oda, Y. Enomoto, M. Suzuki, and T. Murakami, Phys. Rev. B **38**, 6614 (1988).

[4]J. G. Bednorz and K. A. Müller, Z. Phys. B **64**, 189 (1986).

[5]J. D. Axe, D. E. Cox, K. Mohanty, H. Moudden, A. Moodenbaugh, Y. Xu, and T. R. Thurston (unpublished).

[6]G. Aeppli and D. J. Buttrey, Phys. Rev. Lett. **61**, 203 (1988); and (private communication).

[7]R. J. Birgeneau, C. Y. Chen, D. R. Gabble, H. P. Jenssen, M. A. Kastner, C. J. Peters, P. J. Picone, T. Thio, T. R. Thurston, H. L. Tuller, J. D. Axe, P. Böni, and G. Shirane, Phys. Rev. Lett. **59**, 1329 (1987).

[8]P. Böni, J. D. Axe, G. Shirane, R. J. Birgeneau, C. Y. Chen, D. R. Gabbe, H. P. Jenssen, M. A. Kastner, C. J. Peters, P. J. Picone, T. Thio, T. R. Thurston, and H. L. Tuller, Phys. Rev. B **38**, 185 (1988).

[9]G. Heger, D. Mullen, and K. Knorr, Phys. Status Solidi (a) **35**, 627 (1976).

[10]D. Vaknin, S. K. Sinha, D. E. Moncton, D. C. Johnston, J. Newsam, C. F. Safinya, and J. E. King, Jr., Phys. Rev. Lett. **58**, 2802 (1987).

[11]B. Yang, S. Mitsuda, G. Shirane, Y. Yamaguchi, H. Hamaguchi, and Y. Syono, J. Phys. Soc. Jpn. **56**, 2283 (1987).

[12]K. Fukuda, S. Shamoto, M. Sato, and K. Oka, Solid State Commun. **65**, 1323 (1988).

[13]Tineke Thio, T. R. Thurston, N. W. Preyer, P. J. Picone, M. A. Kastner, H. P. Jenssen, D. R. Gabbe, C. Y. Chen, R. J. Birgeneau, and Amnon Aharony, Phys. Rev. B **38**, 905 (1988).

[14]M. A. Kastner, R. J. Birgeneau, T. R. Thurston, P. J. Picone, H. P. Jenssen, D. R. Gabbe, M. Sato, K. Fukuda, S. Shamoto, Y. Endoh, M. Sato, K. Yamada, and G. Shirane, Phys. Rev. B **38**, 6636 (1988).

[15]K. Fukuda, M. Sato, S. Shamoto, M. Onoda, and S. Hosoya, Solid State Commun. **63**, 811 (1987).

[16]K. Yamada, E. Kudo, Y. Endoh, Y. Hidaka, M. Oda, M. Suzuki, and T. Murakami, Solid State Commun. **64**, 753 (1987).

[17]D. B. Buttrey, J. M. Honing, and C. N. R. Rao, J. Solid State Chem. **64**, 287 (1987).

[18]P. Ganguly and Sheela Ramasesha, Magn. Lett. **1**, 131 (1980).

[19]R. A. Mohan Ram, P. Ganguly, and C. N. R. Rao, Mater.

Res. Bull. **23**, 501 (1988).
[20]L. R. Le Coustumer, Y. Barbaux, and J. P. Bonnelle, Nuov. J. Chem. **6**, 7 (1982).
[21]T. Matsuura, J. Mizusaki, S. Yamauchi, and K. Fueki, Jpn. J. Appl. Phys. **23**, 1143 (1984).
[22]T. Matsuura, J. Tabuchi, J. Mizusaki, S. Yamauchi, and K. Fueki (unpublished).
[23]J. J. Janecek and G. P. Wirtz, J. Am. Ceram. Soc. **61**, 242 (1978).
[24]P. Lehuede and M. Daire, C. R. Acad. Sci. (Paris), Ser. C **276**, 1783 (1973).
[25]J. T. Lewandowski, R. A. Beyerlein, J. M. Longo, and R. A. McCauley, J. Am. Ceram. Soc. **69**, 699 (1986).
[26]U. Lehmann and HK. Muller-Buschbaum, Z. Anorg, Allg. Chem. **470**, 59 (1980).
[27]K. Yamada, E. Kudo, Y. Endoh, K. Tsuda, M. Tanaka, K. Kokusho, H. Asano, F. Izumi, Y. Hidaka, M. Suzuki, and T. Murakami (unpublished).
[28]R. J. Birgeneau, H. J. Guggenheim, and G. Shirane, Phys. Rev. B **1**, 2211 (1970).
[29]D. C. Khan and R. A. Erickson, Phys. Rev. B **1**, 2243 (1970).
[30]H. Ikeda, J. Phys. Soc. Jpn. **37**, 660 (1974); H. Ikeda and K. Hirakawa, Solid State Commun. **14**, 529 (1974).
[31]T. Matsuura, J. Tabuchi, J. Mizusaki, S. Yamauchi, and K. Fueki (unpublished).
[32]R. J. Birgeneau, M. A. Kastner, and A. Aharony, Z. Phys. B **71**, 57 (1988).
[33]H. Kamimura, S. Matsuro, and R. Saito, Solid State Commun. **67**, 303 (1988).